Bulgarian Chemical Communications, Volume 50 Special Issue A (pp. 183- 188) 2018

The electrochemical behavior of LiV_3O_8 obtained via different syntheses as negative active material in aqueous Li-ion battery

T. Petkov[1*], T. Stankulov[2], K. Banov[1,2], and A. Momchilov[2]

[1)] University of Chemical Technology and Metallurgy – UCTM, bul. "Kl. Ohridski"8, 1756 Sofia
[2)] Institute of Electrochemistry and Energy Systems "Acad. E. Budevski", Bulgarian Academy of Sciences, Acad. Georgi Bonchev Str., bl. 10, 1113 Sofia, Bulgaria

Received September 11, 2017; Accepted November 16, 2017

The electrochemical properties of the lithium trivanadate (LiV_3O_8, LVO) as a negative electrode material for aqueous Li-ion battery was studied. Two methods of synthesis were applied to prepare LiV_3O_8: sol-gel method followed by solid-state reaction (SSR) at 500 and 550 °C and melting process with subsequent hydrothermal treatment and drying.As a counter electrode was used $LiMn_2O_4$ (LMO) prepared by conventional SSR synthesis. The intercalation/de-intercalation of lithium ions occurs within the window of electrochemical stability of the water. LiV_3O_8 prepared by melting process, hydrothermally treated and dried (MP65DR), shows a poorer performance in galvanostatic mode compared to these obtained via sol-gel. The sample obtained via sol-gel followed by SSR at 550 °C (SG55) shows an initial specific capacities of ~75 (intercalation) and ~52 (de-intercalation) $mAh.g^{-1}$ which is about 4-5 times less in comparison to the capacities delivered in non-aqueous electrolytes. Although the lower capacity (30-33 $mAh.g^{-1}$), the other sol-gel sample annealed at 500 °C (SG50) displays better capacity retention and coulombic efficiency throughout the cycles.

Keywords: Aqueous Li-ion Battery, anode active material, Lithium trivanadate

INTRODUCTION

Li-ion Batteries (LIBs) possess large energy densities but it employs organic electrolytes which consists highly toxic and flammable solvents. Furthermore the electrolyte manufacture is complicated and expensive, partly because it is sensitive to moisture and air. Incorporation of aqueous electrolytes in rechargeable lithium batteries will improve their safety and economical parameters as well as minimization of the environmental issues. Although the aqueous electrolytes are stable in narrower electrochemical window (0-2 V) than their organic counterparts (0-4.5 V), they are much safer, less toxic and easer to manufacture [1]. Dahn and co-workers were one of the first research groups that proposed an aqueous based type battery using b-VO_2 and $LiMn_2O_4$ (LMO) as negative and positive electrodes, respectively [2]. Another aqueous battery system with improved cycling stability that was recently presented is $LiTi_2(PO_4)_3$ | Li_2SO_4 | $LiFePO_4$[3]. G.J. Wang *et al.* studied electrochemical performance of a LiV_3O_8 (negative electrode) and $LiCoO_2$ (positive electrode) in saturated $LiNO_3$ aqueous electrolyte. These two electrode materials are stable in the aqueous solution and the obtained capacity of this cell system is about 55 $mAh\ g^{-1}$ which is comparable to those of the lead acid and Ni–Cd batteries [4]. Lithium trivanadate (LiV_3O_8, LVO) is a compound with layered 2D structure, which was defined by Wadsley as a γ-LiV_3O_8 [5]. LVO is widely investigated as positive active materials for rechargeable non-aqueous Li batteries [6-11]. Its active working window is between 1.5 and 3.5 V vs Li/Li^+. Hydrothermal treatment of the active material leads to an increase of the interlayer distance due to the incorporation of water molecules into the structure [12]. This modification improves the initial electrochemical lithiation of the compound to 320 $mAh\ g^{-1}$, corresponding to ~3.5 Li per mol inserted in LVO. This result correlates with the assumption of Thackeray *et al.* that is possible up to 4 Li^+ to be inserted in LiV_3O_8[13]. Furthermore the reversible (de-intercalation) specific capacity increases to 280 $mAh\ g^{-1}$, which corresponds to 3 Li per mol LVO. After few cycles the reversible capacity fades to 250 $mAh\ g^{-1}$. Theoretically maximum potential difference of about 3V could be reached if LiV_3O_8 is paired with counter electrode of $LiMn_2O_4$.This fact prompts an interest to study such water based battery configuration and its Li^+ intercalation and de-intercalation processes. LVO possesses lower electrochemical potential than LMO thus appears to be negative electrode in the above mentioned system.

The aim of this work is to study the electrochemical properties of LiV_3O_8 obtained via different synthesis approaches and tested as negative

* To whom all correspondence should be sent.
E-mail: todorvp@abv.bg

active material for aqueous rechargeable lithium battery (ARLB).

EXPERIMENTAL

Samples preparation

Lithium trivanadate was synthesized via two ways. Two of the samples were prepared via sol-gel as follows: V_2O_5 (synthesized by decomposition of NH_4VO_3 (Fluka, >99 %) at 320 °C [14]) was added in preliminary prepared water solution of $H_2C_2O_4.2H_2O$ (Neuber GmbH, 99.5%). Separately $LiOH.H_2O$ (Neuber GmbH, 99%) was dissolved in distilled water and added to the main solution after completely dissolution of the vanadium oxide. The molar ratio between the initial compounds $LiOH/V_2O_5/H_2C_2O_4.2H_2O$ was 1/1.5/6. The final solution was constantly stirred and evaporated at ~80 °C until a dry precursor was formed. Then the precursor was annealed at 500 °C for16h under air atmosphere (sample SG50). Part of the product was annealed again at 550 °C for another 16h in air atmosphere (sample SG55). Alternatively, another LiV_3O_8 sample was prepared by mixing stoichiometric amounts of Li_2CO_3 and V_2O_5 and grinding them in a ball-mill for 30 min. Afterwards the homogenized mixture was melted at 650 °C [12]. After cooling down the smelt was ground in a ball-mill for 8h (sample MP65). Then a part of the product was sealed in autoclave and treated hydrothermally at 320 °C for 24h in order to expand the interlayer distances in the structure (sample MP65HT). Finally the powder was dried at 250 °C for 24h (sample MP65DR).

$LiMn_2O_4$ (LMO) was prepared via conventional solid state reaction (SSR) synthesis using stoichiometric amounts of $LiNO_3$ and MnO_2 and annealing temperature at 750 °C. The synthesis is described in details elsewhere [15].

Characterization techniques

Powder X-ray diffraction (XRD) was performed on a Philips APD 15 diffractometer with Cu Kα radiation. Thermogravimetric (TGA) and differential thermal (DTA) analyses of the sol-gel precursor were carried out in air on a Stanton Redcroft STA 780 thermal analyzer, in the range 20–570 °C at a heating rate of 5 K min^{-1}. The morphology of the powders was observed by Scanning Electron Microscopy (SEM) on JEOL 200-CX (MP65 and MP65DR) and Philips525/EDAX 9900 (SG50 and SG55). The evaluation of specific surface area (SSA) was conducted by the Brunauer-Emmett-Teller (BET) method on a Strohlein& Co. Area instrument.

Electrochemical testing

The ARLB system was fabricated in two (galvanostatic mode) and three (cyclic voltammetry) electrode cells. The working electrodes were prepared by mixing an active materials and teflonized acetylene black (TAB) [16] in ratio 1:1, then deposited onto Ni mesh and pressed at 3.0 tones per cm^2. The LiV_3O_8 active material loading was ~14 $mg.cm^{-2}$ and weight ratio between the positive and negative active materials was kept $LiMn_2O_4$:LiV_3O_8 = 3:1 in all cases based on their specific capacities obtained in non-water electrolytes. Ag/AgCl was used as a reference electrode. Saturated solution of 6M $LiNO_3$ (Chimtex Ltd., 99.8%) in distilled water was used as electrolyte for the electrochemical testing. The cycling voltammetry was carried out on Autolab PSTAT 10 instrument at sweep rate 50 μV s^{-1} and voltage range -0.8 to 0V vs Ag/AgCl. The galvanostatic tests were performed on Arbin BT 2000 in the voltage range 0.7 –1.9 V vs. $LiMn_2O_4$, at C/10 (0.1C) and C/100 (0.01C) where C is the theoretical specific capacity for 3 moles of intercalated Li^+ in LiV_3O_8, i.e. ~279.4 mAh g^{-1} and 10 or 100 are the theoretical charge or discharge time in hours.

RESULTS AND DISCUSSIONS

Thermogravimetric and differential thermal analyses were carried out for a precursor obtained after the first step of the sol-gel process, thus after drying (aging) the gel (Fig. 1).

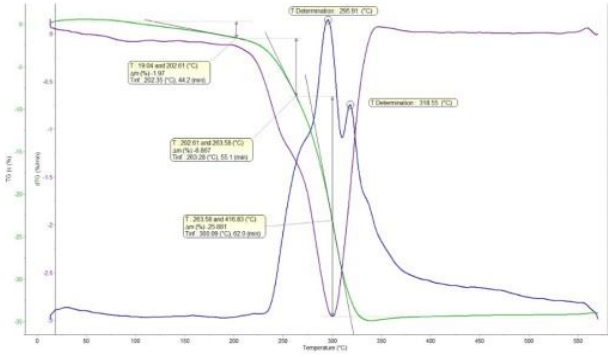

Fig. 1 TG-DTA of the precursor obtained via sol-gel.

The initial weight loss in the range 20-200 °C can be attributed to a small amount of crystal water and/or adsorbed moisture in the precursor. The large weight loss is due to the decomposition of oxalic acid and $LiHC_2O_4$[17]. The strong exothermal peaks in the differential thermogram at ~296 and ~319 °C are caused by the carbon combustion and most likely vanadium oxidation ($V^{4+} \rightarrow V^{5+}$). Heretofore the vanadium was reduced from V^{5+} to V^{4+} (forming VO^{2+} ion) by the oxalic acid during the sol-gel process, a phenomenon that is inevitable during the V_2O_5 dissolution. The small increase of the sample

weight after 330 ˚C could be associated with gaining of oxygen by the sample to complete the synthesis of the product (LiV_3O_8). The small peak at about 570 ˚C is most probably due to some initial melting of the sample. Thus two synthesis temperatures were chosen at 500ºC (sample SG50) and 550ºC (sample SG55).

The XRD patterns of samples prepared via sol-gel method followed by sintering at 500 °C (SG50) and 550 °C (SG55) as well as Wadsley's standard [5] are presented in Fig. 2. The formation of LiV_3O_8 is evident even at 500 °C. Better crystallinity was obtained at 550°C.

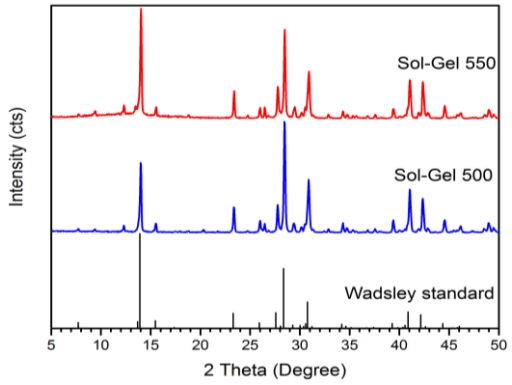

Fig. 2 XRD of the samples prepared via sol-gel method (SG50 and SG55).

There are two additional small peaks in both samples' patterns at 9.3° and 12.3° 2Θ which are not part of the Wadsley's standard. Based on our previous experience we suspect that these peaks are caused by small amount of absorbed water molecules (from the atmosphere) between the structure's layers [12]. This phenomenon is more evident in fig. 3 where such peaks appear at the same positions when the material obtained via meting process is hydrothermally treated (fig. 3b). These peaks vanish when the hydrothermally treated material is dried above 250 °C (Fig. 3c).

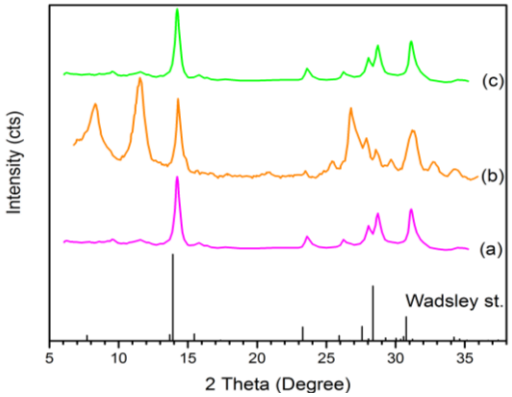

Fig. 3. XRD of samples obtained via melting process: (a) after synthesis (MP65), (b).

Scanning electron microscopy images of melted sample after 8h grinding in a ball-mill (MP65) and hydrothermally treated and dried (MP65DR) are illustrated in Fig. 4.

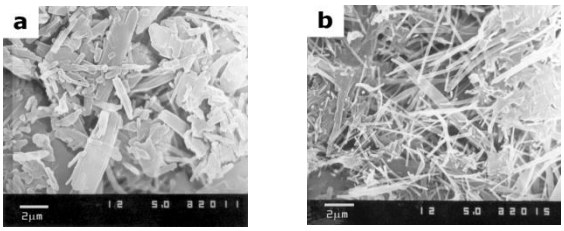

Fig. 4 Scanning electron microscopy of MP65 (a) and MP65DR (b).

The untreated sample shows flake-like type of morphology (fig. 4a). These flakes seem to become fractured into rod-like particles due to the high pressure of the water during the hydrothermal process (fig. 4b). Sample SG50 shows similar morphology of thin rods and flakes (fig. 5 a, c). These rods appear to grow during the additional 16h at 550 °C forming bigger block-like particles/agglomerates presented by SG55 (fig. 5 b, d).

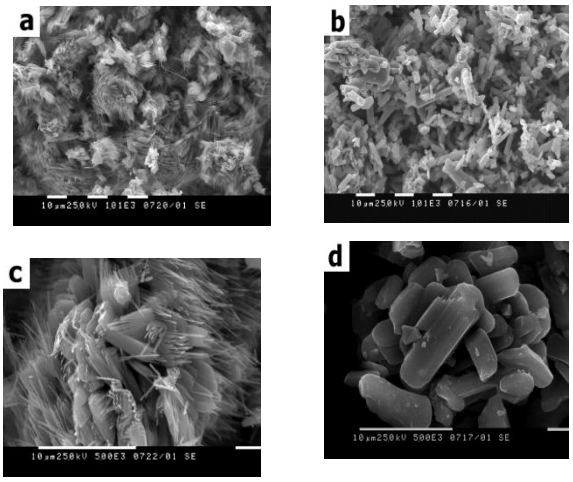

Fig. 5 Scanning electron microscopy of samples SG50 (a and c) and SG55 (b and d).

The specific surface area (SSA) of the materials was evaluated by Brunauer-Emmett-Teller (BET) method. The SSA of MP65 and MP65DR samples are 1.1 and 11 m^2 g^{-1}, respectively, while sol-gel samples display 1.5m^2 g^{-1} (SG50) and 1.1 m^2 g^{-1} (SG55).

The cycling voltammetry (CV) of the materials is shown in Fig. 6. All Li^+ insertion peaks of LiV_3O_8 observed in organic electrolyte [12] seem to be merged in one broad peak split into two apexes at -0.43 and -0.33 V vs Ag/AgCl when sample MP65DR is tested in aqueous electrolyte. Similarly SG50 display one broad cathodic peak (-0.34 V vs Ag/AgCl) in contrast to SG55 showing three distinguished peaks at -0.25, -0.31 and -0.47 V vs

Ag/AgCl. The oxidation curves of SG50 and MP65DR also appear to be similar in shape with two peaks for each sample at -0.35 and -0.19 V vs Ag/AgCl (SG50), and -0.39 and -0.25 V vs Ag/AgCl (MP65DR). SG55 shows three anodic peaks (-0.31, -0.27 and -0.23V vs Ag/AgCl) which are merged into one broad feature during the de-intercalation process. After integration of the areas, the initial delivered intercalation and following de-intercalation capacities are 64.35 and 55.43 mAh g^{-1} (SG50), 92.68 and 67.48 mAh g^{-1} (SG55), and 123.87 and 73.12 mAh g^{-1} (MP65DR), respectively. These capacity values delivered in aqueous electrolyte are much lower in comparison to their organic counterparts (20-50% lower) [12].

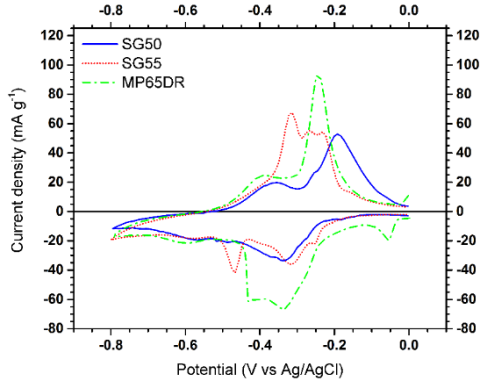

Fig. 6 Cyclic voltammetry of SG50, SG55 and MP65DR at a scan rate of 50 μV s^{-1} in the voltage range of 0 and -0.8 V vs. Ag/AgCl.

Galvanostatic tests were conducted in order to investigate the electrochemical performance of the studied materials. Fig. 7a shows initial charge-discharge profiles of the samples at C/10 (0.1C) in the voltage range 0.7-1.9 V vs $LiMn_2O_4$ (LMO). Both SG50 and SG55 present solid-solution-type (shape) of the de/intercalation curves. These samples deliver 35.45 (SG50) and 75.23 (SG55) mAh g^{-1} during the first lithiation, and 30.57 (SG50) and 51.50 (SG55) mAh g^{-1} in the consecutive de-lithiation process. Although MP65DR delivers the highest capacities in potentiodynamic mode (fig. 6), it performs very poorly in galvanostatic mode, marking 4.2 and 0.3 mAh g^{-1} during first intercalation (Int) and de-intercalation (Dei). Even when the current load is lowered as much as C/100 (fig. 7b), the delivered capacities are unsatisfactory: 47.77 (Int) and 9.8 (Dei) mAh g^{-1}, implying kinetic difficulties thus hindered diffusion.

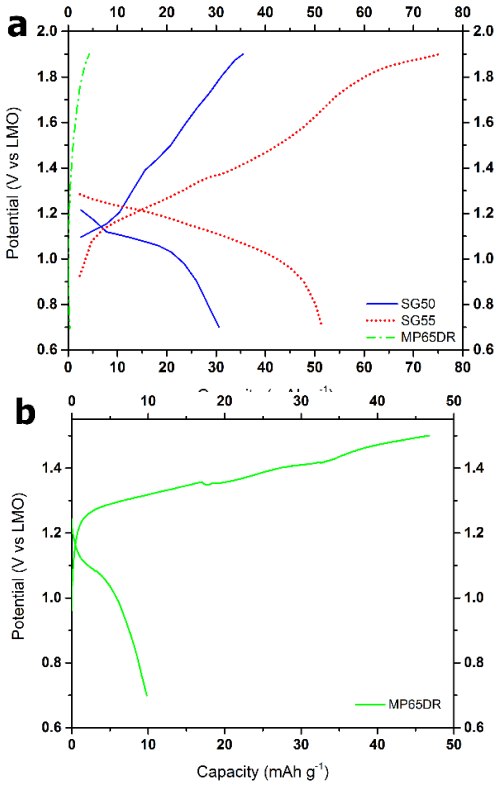

Fig. 7 Galvanostatic tests: (a) charge-discharge profiles of all materials at C/10 in the voltage range 0.7-1.9 V vs LMO; (b) charge-discharge profiles of MP65DR at C/100 in the voltage range 0.7-1.5 V vs LMO.

The de-intercalation specific capacity of the studied materials (discharge mode for the whole LVO-LMO system) as functions of the cycles at C/10 in the voltage range 0.7-1.9 V vs LMO are presented in fig. 8a. SG55 marks highest de-lithiation capacity of ~55 mAh g^{-1} in the 4th cycle. After 10th cycle the materials becomes unstable expressed by fluctuations and rapid capacity loss of ~40% in the 30th cycle (fig. 8b). Although the capacity of SG50 is lower, this material display steady behavior with varying capacity of 30-33 mAh g^{-1}. The capacity retention (fig. 8b) in every cycle is calculated as follows:

$$CapRet = \frac{C_n}{C_1} * 100\ [\%],$$

where C_n and C_1 are the capacities of the respective and first cycles, respectively. Therefore the capacity retention of sample SG50 (2-30 cycles) exceeds 100% due to the lowest capacity (30.57 mAh g^{-1}) is delivered in the first cycle. The coulombic efficiency (95-97% after 4th cycle) of this sample is also much better compared to SG55 (70-90%) (Fig. 8c).

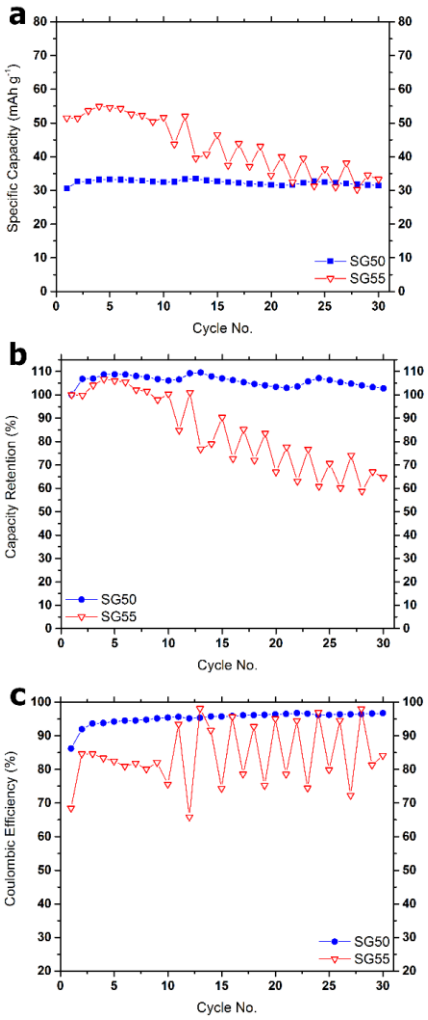

Fig. 8. Specific capacity (a), capacity retention (b) and coulombic efficiency (c) as functions of the cycles at C/10 in the voltage range 0.7-1.9 V vs LMO.

CONCLUSIONS

LiV_3O_8 active materials were synthesized via sol-gel followed by solid state reaction at 500 and 550 °C, and melting process at 650 °C with subsequent hydrothermal treatment and drying. X-ray diffraction patterns show that samples were successfully indexed as LiV_3O_8. However, there are additional small peaks at 9.3° and 12.3° 2Θ in the patterns of SG50 and SG55 which can be attributed to small amounts of absorbed water from the atmosphere. Among all samples SG55 delivers the highest capacities of 75.23 and 51.50 mAh g^{-1} during the first lithiation and de-lithiation, respectively, in galvanostatic mode. However, SG50 appears to be more stable throughout the cycles. Although MP65DR shows highest intercalation and de-intercalation capacities (123.87 and 73.12 mAh g^{-1}) in potentiodynamic mode, this material performs very poorly in galvanostatic mode.

REFERENCES

1. J. Yan, J. Wang, H. Liu, Z. Bakenov, D. Gosselink, P. Chen, *Journal of Power Sources*, **216,** 222 (2012).
2. W. Li, J.R. Dahn, D.S. Wainwright, *Science*, **264**, 1115 (1994).
3. J.-Y. Luo, W.-J. Cui, P. He, Y.-Y. Xia, *Nature Chemistry*, **2**, 760, (2010).
4. G.J. Wang, N.H. Zhao, L.C. Yang, Y.P. Wu, H.Q. Wu, R. Holze, *Electrochimica Acta*, **52,** 4911 (2007).
5. A. Wadsley, *Acta Crystallographica*, **10,** 261 (1957).
6. D.G. Wickham, *Journal of Inorganic and Nuclear Chemistry*, **27,** 1939 (1965).
7. G. Pistola, M. Pasquali, M. Tocci, V. Manev, R.V. Moshtev, *Journal of Power Sources*, **15**, 13-25, (1985).
8. A. Hammou, A. Hammouche, *Electrochimica Acta*, **33(12)**, 1719 (1988).
9. G. Pistoia, M. Pasquali, G. Wang, L. Li, *Journal of The Electrochemical Society*, **137**, 2365 (1990).
10. T. Miyazaki, T. Ogino, Y. Masuda, H. Wada, T. Kawagoe, Patent US5013620A (1991).
11. A. Momchilov, V. Manev, A. Nassalevska, M. Pasquali, G. Pistoia, *Journal of Applied Electrochemistry*, **20**, 763 (1990).
12. V. Manev, A. Momchilov, A. Nassalevska, G. Pistoia, M. Pasquali, *Journal of Power Sources*, **54**, 501 (1995).
13. L. A. de Picciotto, K.T. Adendorff, D.C. Liles, M.M. Thackeray, *Solid State Ionics*, **62**, 297(1993).
14. V. L. Volkov, Sverdlovsk: Ural. Nauchn. Tsentr, Akad. Nauk SSSR, (1987).
15. A. Momchilov, V. Manev, A. Nassalevska, A. Kozawa, *Journal of Power Sources*, **41**, 305(1993).
16. V. Manev, A. Momchilov, K. Tagawa, A. Kozawa, *Progress in Batteries & Battery Materials*, **12**, 157, (1993).
17. D. Li, F. Lian, K.-C. Chou, *Rare Metals*, **31**, 615 (2012).

ЕЛЕКТРОХИМИЧНИ СВОЙСТВА НА LiV_3O_8, ПОЛУЧЕН ЧРЕЗ РАЗЛИЧНИ МЕТОДИ НА СИНТЕЗ, КАТО ОТРИЦАТЕЛЕН АКТИВЕН МАТЕРИАЛ В ЛИТИЕВО-ЙОННА БАТЕРИЯ С ВОДЕН ЕЛЕКТРОЛИТ

Т. Перков[1*], Т. Станкулов[2], К. Банов[1,2], А. Момчилов[2]

[1]Химикотехнологичен и металургичен университет, бул. "Климент Охридски" 8, 1756 София, България
[2]Институт по електрохимия и енергийни системи, Българска академия на науките, ул. "Акад. Георги Бончев" бул. 10, 1113 София, България

Постъпила на 11 септември, 2017 г.; приета на 16 ноември, 2017 г.

(Резюме)

Изследвани са електрохимичните свойства на литиевия триванадат (LiV_3O_8, LVO) като отрицателен електроден материал за литиево-йонна батерия с воден електролит. Два метода на синтез бяха приложени за подготовка на LiV_3O_8: метод зол-гел, последван от реакция в твърдофазен синтез (SSR) при 500 и 550°C и процес на топене с последващо хидротермично третиране и сушене. Като за противоелектрод беше използван $LiMn_2O_4$ (LMO), получен чрез конвенционален твърдофазен синтез. Интеркалирането / деинтеркалирането на литиевия йон се извършва в прозореца на електрохимичната стабилност на водата. LiV_3O_8, получен по метода на топене, третиран хидротермично и изсушен (MP65DR), показва по-лошо представяне в галваностатичен режим в сравнение с тези, получени чрез сол-гел. Пробата, получена чрез зол-гел, накалена при 550°C (SG55), показва първоначален специфичен капацитет от ~ 75 (интеркалация) и ~ 52 (де-интеркалация) mAh.g-1, който е около 4-5 пъти по-нисък в сравнение с капацитета, в неводни електролити. Въпреки че е с по-малък капацитет (30-33 mAh.g-1), другата проба от сол-гел, нагрята при 500 ° C (SG50), показва по-добро запазване на капацитета и ефективност при циклите.

Ключови думи: водна литиево-йонна батерия, аноден активен материал, литиев триванадат